JOURNAL OF MAGNETIC RESONANCE, Series A 110, 257–261 (1994)

Measurement of Two- and Three-Bond ^1H–^{13}C J Couplings from Quantitative Heteronuclear J Correlation for Molecules with Overlapping ^1H Resonances, Using t_1 Noise Reduction

GUANG ZHU,* ALISTAIR RENWICK,† AND AD BAX‡§

*Department of Electrical Engineering, University of Maryland, College Park, Maryland 20742; †International Medical College, 21 Jalan Selangor, 46050 Petaling Jaya, Selangor, Malaysia; and ‡Laboratory of Chemical Physics, National Institutes of Diabetes and Digestive and Kidney Diseases, National Institutes of Health, Bethesda, Maryland 20892

Received July 13, 1994

A large variety of different 2D and 3D techniques have been proposed in recent years for measuring long-range ^1H–^{13}C J couplings (*1–17*). In all of these methods the J coupling is measured either from the J_{CH} splitting observed in the ^{13}C or ^1H multiplet or from the E.COSY-type (*18*) displacement of the two components of a multiplet. Recently, a different type of measurement, commonly referred to as quantitative J correlation (*19*), has been introduced for the measurement of a large range of J couplings, including ^{13}C–^{13}C (*20, 21*), ^1H–^{113}Cd, ^1H–^{199}Hg (*22*), ^{13}C–^{15}N (*23*), ^{13}C–^1H (*24*), and ^1H–^1H (*25*) couplings. In previous applications of quantitative J correlation, the long-range J_{CH} values were derived from the ratio of intensities observed in a HMBC 2D spectrum and a pseudo-2D reference spectrum (*24*). In the F_1 dimension of this pseudo-2D reference spectrum, the resonances are all located at $F_1 = 0$ and exhibit a multiplet shape that is similar to that observed in the 2D HMBC spectrum. For molecules with extensive overlap in the 1D ^1H spectrum this method does not function satisfactorily because the 1D overlap is not resolved in the pseudo-2D reference spectrum. Here we describe a slightly different approach, where the reference spectrum is a true 2D spectrum, with ^1H resonances dispersed in the F_1 dimension by the ^{13}C chemical shift of their directly attached ^{13}C nucleus.

The pulse scheme used in the present work is shown in Fig. 1. The intensity of a ^1H–^{13}C correlation in the 2D spectrum is, to a good approximation, proportional to $\sin^2[\pi J(T - 2\Delta)]$. Keeping T constant (approximately 40 ms), two spectra are recorded: a reference spectrum with $\Delta = T/2 - 1/(4\,^1J_{CH})$, and a long-range correlation spectrum with $\Delta = 0$. Homonuclear ^1H–^1H dephasing is active for a time $2T + t_1$ both in the reference and in the long-range correlation spectra and therefore, to first order, does not affect the intensity ratio. Temporarily neglecting differences in relaxation rates of protons attached to ^{13}C versus ^{12}C, the intensity ratio of the long-range correlation to a carbon X (I_{HX}) and the one-bond correlation intensity in the reference spectrum (I_{HC}) is then given by

$$I_{HX}/I_{HC} = (N_{lr}/N_{ref})\sin^2(\pi T J_{HX}), \qquad [1]$$

where J_{HX} is the size of the long-range correlation between the observed proton and carbon X, and (N_{lr}/N_{ref}) is the ratio of the number of scans in the long-range and in the reference spectrum. Equation [1] assumes that for the reference spectrum the condition $\sin^2[\pi\,^1J_{HC}(T - 2\Delta)] = 1$ applies, where $^1J_{HC}$ is the one-bond J_{CH} coupling. Although this condition is satisfied for only a single value of $^1J_{HC}$, changes by up to 10% have only very small effects (<2.5%) on the intensity ratio of Eq. [1], allowing J_{HX} to be derived from

$$J_{HX} = (\pi T)^{-1}\sin^{-1}[\sqrt{(I_{HX}N_{ref})/(I_{HC}N_{lr})}]. \qquad [2]$$

Dephasing due to homonuclear ^1H–^1H coupling is identical in the reference and in the long-range correlation experiments, and multiplet shapes are expected to be the same in both spectra. In practice, however, small differences in the shape of the cross peak can occur due to (a) strong coupling among the protons, (b) additional line broadening of protons attached to ^{13}C caused by the large one-bond ^1H–^{13}C dipolar interaction, and (c) incomplete ^{13}C decoupling, which is more severe for the one-bond than for the long-range correlations. Of these effects, the difference caused by strong coupling is the most difficult to deal with. Note that two J-coupled protons that differ in chemical shift by about 75 Hz (i.e., by $\sim {}^1J_{CH}/2$) behave like weakly coupled spins if neither one of these two protons is directly attached to ^{13}C. However, in the reference spectrum, only protons attached to ^{13}C are observed and half of the ^1H–$\{^{13}C\}$ doublet would overlap with the resonance of the second proton, distorting ^1H–^1H J modulation during the period $2T + t_1$. Similarly, two J-coupled protons with identical chemical shifts will behave like weakly coupled spins in the one-bond ref-

§ To whom reprint requests should be addressed.

1064-1858/94 $6.00

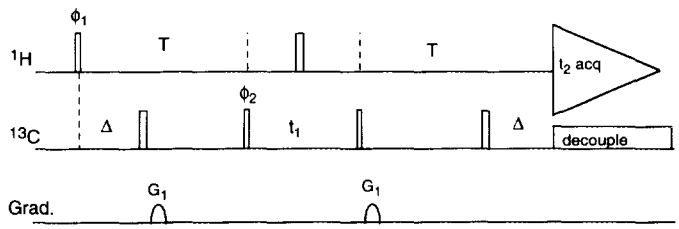

FIG. 1. Pulse scheme of the quantitative HMBC experiment. The reference spectrum, containing exclusively one-bond interactions, is obtained by using $\Delta = T/2 - 1/(4^1J_{CH})$. The long-range correlation spectrum is recorded with the same value for T (typically in the range 30–60 ms), but with $\Delta = 0$. Narrow and wide bars represent 90° and 180° pulses, respectively. The ^{13}C 180° pulses are of the composite type ($90^\circ_x 220^\circ_y 90^\circ_x$). The gradient pulses, G_1, have a duration of 1 ms and have a sine-bell amplitude profile with a maximum strength of 25 G/cm. Phase cycling is as follows: ϕ_1 = $2(x), 2(-x)$; $\phi_2 = x, -x$; receiver = $x, 2(-x), x$.

erence spectrum, but will show strong coupling effects and distorted J_{HH} modulation in the long-range correlation spectrum. As will be discussed later, distortions due to strong coupling are easily recognized, and, in the present work, we do not attempt to derive long-range J coupling information for these protons. Incomplete ^{13}C decoupling and ^{13}C–^{1}H dipolar interactions during t_2 simply cause broadening of the one-bond correlation in the reference spectrum, without affecting the cross-peak integral, and therefore do not prevent the measurement of the relative intensities. The effect of heteronuclear dipolar interactions during the recovery delay and during the period $2T$ cannot be ignored and will be discussed later.

Although a reasonable estimate for I_{HX}/I_{HC} can be obtained from simple peak picking, a better value for $a = I_{HX}/I_{HC}$ can be derived by searching for a, m, and n values that minimize the function

$$f(a, m, n) = \sum_{i,j} [(S^{lr}(i,j) - aS^{ref}(i+m, j+n)]^2, \quad [3]$$

where $S^{lr}(i,j)$ represents a small region of the 2D data matrix containing the long-range correlation for a given HX pair, and $S^{ref}(i+m, j+n)$ is the region of the reference spectrum containing the corresponding one-bond correlation. A small difference in F_2 position of the one-bond versus the long-range correlation, caused by the one-bond ^{1}H–{^{13}C} isotope shift, is adjusted for by optimizing the value of n. The difference in ^{13}C frequency between the two correlations corresponds to m. For each value of m and n, the value of a is calculated by singular-value decomposition (SVD). The optimal value of a is then determined by conducting a grid search over m and n, after initial estimates based on the frequency coordinates of the two resonances involved. Extensive zero filling of the time-domain data, in practice at least eightfold in each dimension, is needed for matching the peak positions with sufficient accuracy. An estimate for the uncertainty in a, Δa, is obtained from

$$\Delta a = \left\{ \frac{\sum_{i,j} [S^{lr}(i,j) - aS^{ref}(i+m, j+n)]^2}{\sum_{i,j} |S^{ref}(i+m, j+n)|^2} \right\}^{1/2}, \quad [4]$$

where the optimal values for m, n, and a, derived in the manner described above, are substituted in the right-hand side of Eq. [4]. Note that although a small difference in F_2 linewidth between the long-range and the one-bond correlations can give rise to a significant increase in Δa, to first order the value found for a is not affected, and Δa is therefore expected to represent an upper limit for the error in a.

A second source of error in the I_{HX}/I_{HC} ratio stems from the difference in T_1 and T_2 relaxation of ^{13}C- and ^{12}C-attached protons during the delay between scans and during the relatively long de- and rephasing periods, T. Protons attached to ^{12}C have longer T_1 values than ^{13}C-attached protons. In practice, the delay between scans is not much longer than the T_1 of many of the ^{12}C-attached protons, resulting in a decrease of I_{HX}/I_{HC}. Faster T_2 relaxation of the ^{13}C-attached protons during the de- and rephasing periods, T, has the opposite effect, resulting in an increase of I_{HX}/I_{HC}. As outlined below, the relative importance of each effect can be estimated easily from simple 1D experiments.

For simplicity we assume that the delay between scans, τ, is at least three times longer than the short T_1 of a ^{13}C-attached proton. Therefore, the ^{13}C-attached protons, which give rise to the reference intensity I_{HC}, may be considered at thermal equilibrium at the beginning of the pulse sequence. If the T_1 value of the ^{12}C-attached proton is $T_{1,^{12}C}$, this proton has relaxed to a fraction of its thermal equilibrium value, resulting in an underestimate of I_{HX}/I_{HC} by a factor $1\text{-}\exp(-\tau/T_{1,^{12}C})$. For resolved ^{1}H resonances, $T_{1,^{12}C}$ is easily measured using standard inversion–recovery experiments. For unresolved resonances, a reasonable estimate for $T_{1,^{12}C}$ frequently can be made on the basis of the T_1 values measured for the resolved protons.

For measuring the difference in transverse relaxation rates of ^{12}C- and ^{13}C-attached protons, we use the following simple procedure. First, two 1D experiments are recorded with the pulse sequence

$$^1\text{H: } 90^\circ_\phi — 1/(2^1J_{CH}) — 180^\circ_x — 1/(2^1J_{CH}) — \text{Acq}_\psi,$$
$$^{13}\text{C: } \qquad 180^\circ_{on/off} \qquad \text{Decouple} \quad [A]$$

with $\phi = x, y, -x, -y$ and $\psi = x, -y, -x, y$. The signal recorded with the 180° ^{13}C pulse, S_{on}, is stored separately from the signal recorded with the ^{13}C pulse off, S_{off}. The ratio $R = (S_{off} - S_{on})/(S_{off} + S_{on})$ is calculated and is typically found to be close to the natural abundance of ^{13}C, i.e., ~1%. Next, the experiment is repeated with longer delay periods, similar to the scheme of Fig. 1,

$$\begin{array}{lll} {}^1\mathrm{H}\text{: } 90^\circ_\phi\text{—}T/2\text{—} & \text{—}T/2\text{—}1/(2\,{}^1J_{\mathrm{CH}})\text{—}180^\circ_x\text{—} & \\ {}^{13}\mathrm{C}\text{:} \quad 90^\circ_x 220^\circ_y 90^\circ_x & 180^\circ_{\mathrm{on/off}} & \\ 1/(2\,{}^1J_{\mathrm{CH}})\text{—}T/2\text{—} & \text{—}T/2\text{—}\ \mathrm{Acq}_\psi, & \\ 90^\circ_x 220^\circ_y 90^\circ_x & \text{Decouple} & [\mathrm{B}] \end{array}$$

where the composite $90^\circ_x 220^\circ_y 90^\circ_x$ is a compromise composite pulse which compensates reasonably well for both resonance offset and RF inhomogeneity (*26*), and T is typically set to the same duration as that used in the pulse scheme of Fig. 1. The intensity ratio, R', is again measured in the same manner as for scheme [A]. Assuming the molecule is rigid and tumbling isotropically, the R'/R ratio is expected to be a constant across the entire ^{1}H spectrum. For the trisaccharide used in the present study R'/R was found to fall in the 0.74 ± 0.08 range when using $T = 40$ ms, suggesting a ^{1}H–$\{^{13}\mathrm{C}\}$ dipolar line broadening of 1.2 Hz. This degree of line broadening corresponds to a rotational correlation time of approximately 250 ps and is close to the value expected for a trisaccharide in D_2O at 25°C.

Both factors discussed above are accounted for when deriving $J_{\mathrm{H}X}$ by modifying Eq. [2]:

$$J_{\mathrm{H}X} = (\pi T)^{-1} \times \sin^{-1}\left\{ \sqrt{\frac{I_{\mathrm{H}X} R' N_{\mathrm{ref}}}{R[1 - \exp(-\tau/T_{1,^{12}\mathrm{C}})] I_{\mathrm{HC}} N_{\mathrm{lr}}}} \right\}. \quad [5]$$

The procedure described above has been used to measure long-range ^{1}H–^{13}C J couplings in the trisaccharide sialyl-α(2-6)-lactose, containing *N*-acetyl-D-neuraminic acid (NAc), galactose (Gal), and glucose (Glc). The glucose unit is a mixture of α (30%) and β (70%) anomers. As discussed above, two 2D spectra need to be recorded: a reference spectrum with $\Delta = 18.4$ ms and $T = 40$ ms, and the long-range correlation spectrum with $\Delta = 0$ and $T = 40$ ms. The reference spectrum results from 32 scans per complex t_1 increment whereas 128 scans per increment were recorded for the long-range correlation spectrum, with a delay time of 1.8 s between scans in both cases.

For both the reference and the long-range correlation spectra, data recorded with $\phi_2 = x$ (odd-numbered FIDs) and $\phi_2 = -x$ (even-numbered FIDs) were stored separately. This allows minimization of t_1 noise in a manner that is conceptually analogous to the t_1-noise-reduction routine proposed by Morris and Cowburn (*27*). In our case, the spectra derived from the odd (S_{odd}) and even-numbered FIDs (S_{even}) are compared, and a complex number k is calculated that minimizes their difference over a small region of the spectrum that contains signals of a resonance not coupled to ^{13}C. In the present case, the residual HDO resonance is chosen for this purpose. The factor k is calculated using SVD by minimizing

$$\sum_{f_2} [S_{\mathrm{odd}}(t_1, f_2) - k S_{\mathrm{even}}(t_1, f_2)]^2, \quad [6]$$

where the summation extends over the small spectral region that contains the HDO resonance. Subsequently a new matrix is calculated from

$$S_{\mathrm{new}}(t_1, f_2) = S_{\mathrm{odd}}(t_1, f_2) - k S_{\mathrm{even}}(t_1, f_2), \quad [7]$$

prior to digital filtering and Fourier transformation in the t_1 dimension. Note that the summation in Eq. [6] does not need to extend over a region that is more than the linewidth of the chosen reference signal, which makes the method easy to apply in cases where the reference line (HDO) is close to resonances of interest. This approach is also applicable if a ^{13}C-attached proton resonance is chosen as a reference. For example, the residual proton solvent peak in a chloroform solution can be used. In the latter case, after making the correction described above, all nonchloroform protons will show a weak spurious correlation to the chloroform ^{13}C resonance, however. Fortunately these artifactual resonances rarely interfere with resonances of interest. On our spectrometer system, application of the very simple correction procedure results in a reduction in t_1 noise by a factor of three.

Compared in Fig. 2 are the most crowded regions of the one-bond and long-range correlation spectra, obtained for unlabeled sialyl-α(2-6)-lactose. For convenience, the spectral window in the ^{13}C dimension has been set to 33 ppm, resulting in aliasing of resonances outside of the 33 ppm window. Because the first t_1 increment has been set to half a dwell time, all resonances that are aliased an odd number of times are of opposite phase to ^{13}C resonances that fall within the spectral window (*28*).

A total of nearly three dozen long-range ^{1}H–^{13}C coupling constants could be measured in the manner described above. These values are reported in Table 1. The majority of these correspond to couplings over two and three chemical bonds. However, a weak correlation that can only be ascribed to a four-bond J coupling is observed between NAc-H7 and NAc-C2. The intensity of this correlation indicates a coupling constant of 1.2 ± 0.3 Hz. The reason for the unusually large value of this four-bond J coupling remains unclear. The J values reported in Table 1 have been corrected for insufficiently long delays between scans, and for the difference in T_2 of ^{13}C- and ^{12}C-attached protons, using the scaling factor of Eq. [5]. The errors reported in Table 1 are based on Eq. [4] and include a 10% uncertainty in the value of the scaling factor, R/R', used in Eq. [5].

Spurious resonances caused by strong ^{1}H–^{1}H coupling in the reference spectrum (Fig. 2A) are marked with a ×. For example, at the left-bottom side of Fig. 2A a strong coupling artifact can be seen that is due to an interaction between Gal-H6R and Gal-H5. A similar artifact is observed at the F_1 frequency of Gal-C6 and the F_2 frequency of Gal-H5.

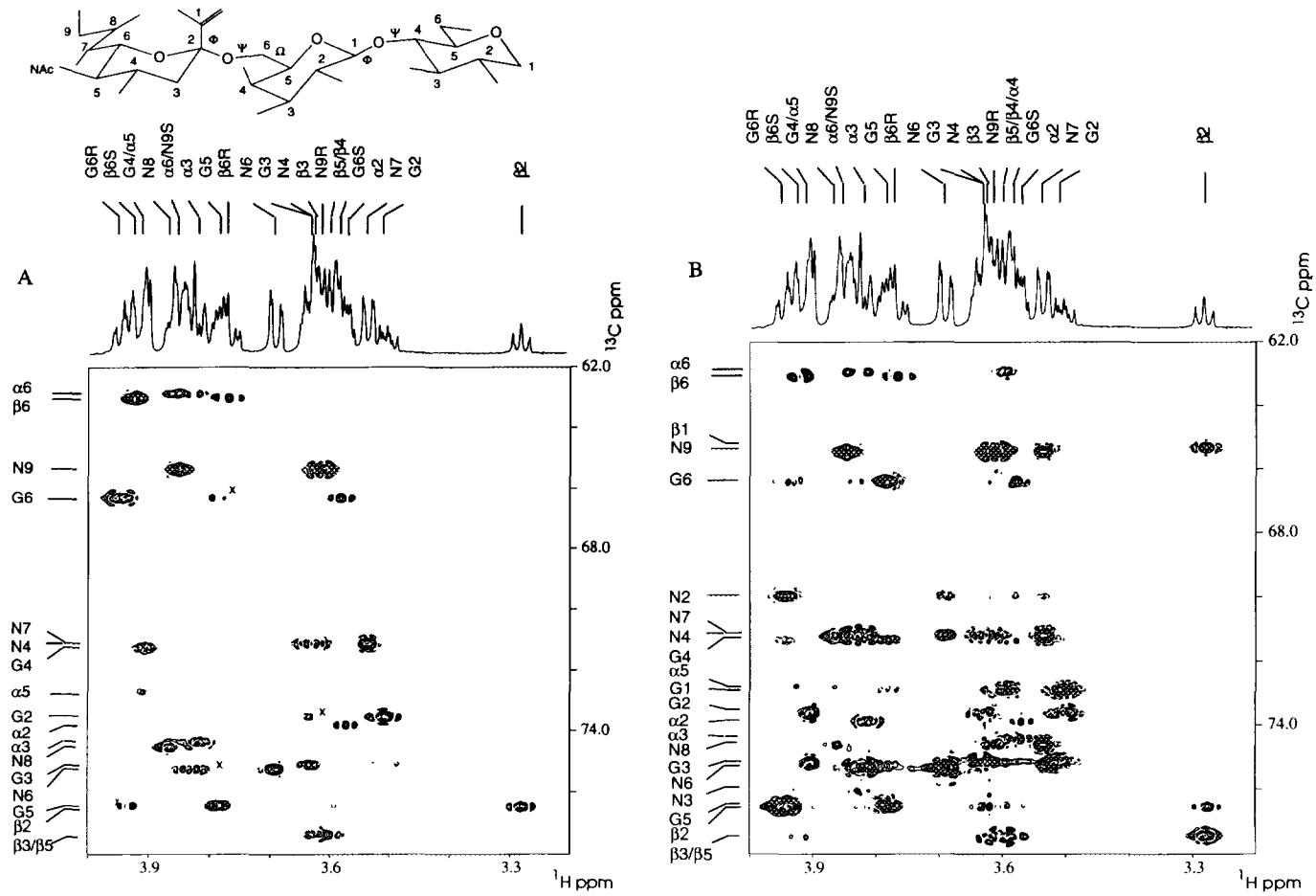

FIG. 2. Small regions of the ^{1}H–^{13}C correlation spectra recorded for sialyl-α(2-6)-lactose and optimized (A) for one-bond J interactions (T = 40 ms, Δ = 19.4 ms) and (B) for long-range connectivity (T = 40 ms, Δ = 0 ms). Experiments are carried out on a 6 mg sample in 0.45 ml D_2O, using a Bruker AMX-600 spectrometer, equipped with a pulsed-field-gradient accessory and a ^{1}H/^{13}C/^{15}N triple-resonance probehead, optimized for ^{1}H detection. Spectra result from 512* × 256* data matrices (n* refers to n complex data points), with acquisition times of 12.8 (t_1) and 85 ms. Data are zero filled to yield a digital resolution of 2.44 (F_1) and 0.74 Hz (F_2). Total measuring times were 4.5 and 18 hours for spectra (A) and (B), respectively. Resonance assignments are indicated along the axes of the 2D spectra; α and β refer to the glucose α- and β-anomers, G to galactose, and N to neuraminic acid. Dashed and solid contours correspond to positive and negative intensities, respectively. The sign of the resonance is determined by the number of times the data have been aliased in the ^{13}C dimension and by the ^{1}H–^{1}H J modulation during the de- and rephasing intervals, T. Spurious resonances caused by strong ^{1}H–^{1}H coupling in the reference spectrum (A) are marked with a ×.

The one-bond reference-peak intensity and lineshape are therefore less reliable in such cases, increasing the uncertainty in the corresponding coupling-constant measurements.

Due to the multitude of long-range interactions and the narrow range of ^{1}H and ^{13}C chemical shifts in carbohydrates, some overlap occurs in the long-range correlation spectrum of Fig. 2B. For example, the Gal-H2/Gal-C3 and NAc-H7/NAc-C6 correlations (at F_2 = 3.52 ppm) partially overlap, making precise measurement of the corresponding coupling constants impossible, even though it is clear from the intensities of the two cross peaks that both long-range J couplings are quite substantial. Only one case of overlap could have been avoided by choosing a different F_1 spectral width: Due to aliasing, the resonances of Gal-C1 and Glc$^{\alpha}$-C5 nearly overlap (at F_1 = 72.7 ppm), prohibiting reliable measurement of the J couplings of these two carbons to Glc$^{\alpha}$-H4.

Upon completion of the measurement of the J values reported in Table 1, we became aware that several ^{1}H–^{13}C J values for the same trisaccharide recently had been reported by Poppe *et al.* (*29*), using a quite different measuring method. The agreement between the two sets (rmsd, 0.5 Hz) is significantly better than expected on the basis of the error reported in Table 1, suggesting that Eq. [4] overestimates the true error of the measurement.

We have demonstrated a method for measurement of long-range ^{1}H–^{13}C J couplings that is applicable to natural-abundance ^{13}C compounds, even when the ^{1}H spectrum shows considerable overlap. Values as small as 1 Hz can be measured provided the sample is sufficiently concentrated (approximately 25 mM in the present work). Measurement of heteronuclear long-range J couplings from such spectra provides valuable structural constraints, complementing dihe-

TABLE 1
Long-Range J Couplings in Sialyl-α(2-6)-lactose (Hz)

Nuclei	J	A^a
$Glc^{\alpha}H_1$–$Glc^{\alpha}C_5$	6.5 ± 0.9[b]	1.36
$Glc^{\alpha}H_1$–$Glc^{\alpha}C_3$	5.3 ± 0.8	1.36
$Glc^{\alpha}H_3$–$Glc^{\alpha}C_4$	2.8 ± 0.5	0.90
$Glc^{\alpha}H_3$–$Glc^{\alpha}C_2$	3.4 ± 0.6	0.90
$Glc^{\alpha}H_6$–$Glc^{\alpha}C_4$	2.9 ± 0.9	0.77
$Glc^{\beta}H_1$–$Glc^{\beta}C_3$	1.2 ± 0.2	1.07[c]
$Glc^{\beta}H_1$–$Glc^{\beta}C_5$	1.2 ± 0.2	1.07[c]
$Glc^{\beta}H_2$–$Glc^{\beta}C_3$	6.5 ± 1.0	1.50
$Glc^{\beta}H_2$–$Glc^{\beta}C_1$	6.1 ± 0.3	1.50
$Glc^{\beta}H_{6R}$–$Glc^{\beta}C_5$	<0.8[d]	
$Glc^{\beta}H_{6S}$–$Glc^{\beta}C_4$	2.5 ± 0.4	0.77
$Glc^{\beta}H_{6S}$–$Glc^{\beta}C_5$	1.4 ± 0.4	0.77
$GalH_{6S}$–$NAcC_2$	1.9 ± 0.5	0.77
$GalH_1$–$GalC_2$	2.2 ± 0.7	0.81
$GalH_1$–$GalC_3$	2.5 ± 0.8	0.81
$GalH_1$–$GalC_5$	1.0 ± 0.2	0.81
$GalH_1$–$Glc^{\alpha/\beta}C_4$	3.9 ± 0.8	0.81
$GalH_2$–$GalC_1$	6.7 ± 1.3	1.56
$GalH_4$–$GalC_2$	5.9 ± 1.4	1.00
$GalH_4$–$GalC_3$	5.1 ± 1.4	1.00
$GalH_{6R}$–$NAclC_2$	3.0 ± 0.3	0.77
$GalH_{6R}$–$CalC_4$	1.8 ± 0.2	0.77
$GalH_{6R}$–$CalC_5$	5.2 ± 1.0	0.77
$NAcH_5$–$NAcC_7$	4.7 ± 0.8	0.90
$NAcH_6$–$NAcC_2$	1.9 ± 0.4	0.99
$NAcH_6$–$NAcC_7$	3.1 ± 0.6	0.99
$NAcH_7$–$NAcC_2$	1.2 ± 0.4	0.90
$NAcH_7$–$NAcC_8$	4.0 ± 0.4	0.90
$NAcH_7$–$NAcC_9$	3.6 ± 0.3	0.90
$NAcH_{3eq}$–$NAcC_1$	<0.9[d]	
$NAcH_{3eq}$–$NAcC_2$	5.2 ± 0.4	0.77
$NAcH_{3eq}$–$NAcC_4$	6.5 ± 0.4	0.77
$NAcH_{3eq}$–$NAcC_5$	9.2 ± 1.7	0.77
$NAcH_{3ax}$–$NAcC_1$	6.0 ± 0.9	0.77
$NAcH_{3ax}$–$NAcC_2$	10.3 ± 1.8	0.77
$NAcH_{3ax}$–$NAcC_4$	7.7 ± 1.1	0.77
$NAcH_{3ax}$–$NAcC_5$	2.7 ± 0.3	0.77

[a] Scale factor for long-range correlation intensity prior to comparison with one-bond correlation, in order to account for differences in ^1H–$\{^{13}C\}$ and ^1H–$\{^{12}C\}$ T_2 and T_1.

[b] The error estimate is based on Eq. [4], and an additional 10% error in the intensity ratio has been added to account for the uncertainty of the scaling factor, A.

[c] Correlations to Glc^{β}–C_3 and –C_5 overlap. The J values reported are based on the assumption that both three-bond J values contribute equally to the observed cross peak.

[d] Upper limit, based on the absence of a cross peak above the noise level.

dral-angle information available from ^1H–^1H J couplings and NOE cross-relaxation rates. This information is particularly valuable when studying flexible molecules, such as carbohydrates and peptides, where the solution conformation is invariably underdetermined. The method described for reducing the t_1 noise in the HMBC spectrum is simple, fast, and remarkably robust, and significantly improves the quality of the spectrum.

ACKNOWLEDGMENTS

We thank Stephan Grzesiek, David Live, Geerten Vuister, and Andy Wang for stimulating discussions. This work was supported by the AIDS Targeted Anti-Viral Program of the Office of the Director of the National Institutes of Health. G.Z. acknowledges support from NIH Grant GM49707.

REFERENCES

1. A. Bax and R. Freeman, *J. Am. Chem. Soc.* **104,** 1099 (1982).
2. H. Kessler, U. Anders, and G. Gemmecker, *J. Magn. Reson.* **78,** 382 (1988).
3. J. Keeler, D. Neuhaus, and J. J. Titman, *Chem. Phys. Lett.* **146,** 545 (1988).
4. W. Bermel, K. Wagner, and C. Griesinger, *J. Magn. Reson.* **83,** 223 (1989).
5. M. Ochs and S. Berger, *Magn. Reson. Chem.* **28,** 994 (1990).
6. L. Poppe and H. van Halbeek, *J. Magn. Reson.* **92,** 636 (1991).
7. L. Poppe and H. van Halbeek, *J. Magn. Reson.* **93,** 214 (1991).
8. J. M. Richardson, J. J. Titman, J. Keeler, and D. Neuhaus, *J. Magn. Reson.* **93,** 533 (1991).
9. B. Adams and L. E. Lerner, *J. Magn. Reson. A* **103,** 97 (1993).
10. G. T. Montelione, M. E. Winkler, P. Rauenbuehler, and G. Wagner, *J. Magn. Reson.* **85,** 426 (1989).
11. A. S. Edison, W. M. Westler, and J. L. Markley, *J. Magn. Reson.* **92,** 434 (1991).
12. P. Schmieder, M. Kurz, and H. Kessler, *J. Biomol. NMR* **1,** 403 (1991).
13. E. R. P. Zuiderweg and S. W. Fesik, *J. Magn. Reson.* **93,** 653 (1991).
14. U. Wollborn and D. Leibfritz, *J. Magn. Reson.* **98,** 142 (1992).
15. U. Eggenberger, Y. Karimi-Nejad, H. Thüring, H. Rüterjans, and C. Griesinger, *J. Biomol. NMR* **2,** 583 (1992).
16. M. Sattler, H. Schwalbe, and C. Griesinger, *J. Am. Chem. Soc.* **114,** 1126 (1992).
17. G. W. Vuister and A. Bax, *J. Biomol. NMR* **2,** 401 (1992).
18. C. Griesinger, O. W. Sørenson, and R. R. Ernst, *J. Chem. Phys.* **85,** 6837 (1986).
19. A. Bax, G. W. Vuister, S. Grzesiek, F. Delaglio, A. C. Wang, R. Tschudin, and G. Zhu, *Methods Enzymol.* **239,** 79 (1994).
20. A. Bax, D. Max, and D. Zax, *J. Am. Chem. Soc.* **114,** 6923 (1992).
21. S. Grzesiek, G. W. Vuister, and A. Bax, *J. Biomol. NMR* **3,** 487 (1993).
22. P. R. Blake, M. F. Summers, M. W. W. Adams, J.-B. Park, Z. H. Zhou, and A. Bax, *J. Biomol. NMR* **2,** 527 (1992).
23. G. W. Vuister, A. C. Wang, and A. Bax, *J. Am. Chem. Soc.* **115,** 5334 (1993).
24. G. Zhu and A. Bax, *J. Magn. Reson. A* **104,** 353 (1993).
25. G. W. Vuister and A. Bax, *J. Am. Chem. Soc.* **115,** 7772 (1993).
26. R. Freeman, S. P. Kempsell, and M. H. Levitt, *J. Magn. Reson.* **38,** 453 (1980).
27. A. Gibbs, G. A. Morris, A. G. Swanson, and D. Cowburn, *J. Magn. Reson. A* **101,** 351 (1993).
28. A. Bax, M. Ikura, L. E. Kay, and G. Zhu, *J. Magn. Reson.* **91,** 174 (1991).
29. L. Poppe, R. Stuike-Prill, B. Meyer, and H. van Halbeek, *J. Biomol. NMR* **2,** 109 (1992).